Kinematic and Dynamic Analysis of Baxter Arm

Abhinav Gandhi[1], Archit Kumar[1] and Snehal Dikhale[1]

***Abstract*— The Baxter robot is a collaborative robot with two redundant serial manipulators as arms. Each of its arms has seven degrees of freedom, including three offsets. We seek to implement what we have studied so far in RBE 501-Robot Dynamics on the left arm of the Baxter robot. The forward and inverse kinematics along with the velocity kinematics is performed which gives us the kinematic solution of the robot. This is followed by the formulation of the dynamic model of the left serial manipulator. Additionally we perform an experiment wherein we verify our kinematic solution by comparing our calculations with the real time values read from the robot encoders.**

Keywords: Baxter robot, serial manipulator, kinematics, dynamic model

I. INTRODUCTION

The Baxter Robot, a product by Rethink Robotics, is an anthropomorphic serial manipulator on a mobile platform with seven Degrees of Freedom (DoF) on each of its two arms, a two DoF head, and a torso with a mobile platform. The arms are actuated by Series Elastic Actuators (SEA) which incorporate torsional springs and thus allow some compliance. This feature along with various software features render the Baxter Robot, human-friendly and hence extremely popular for research activities. The servo motors also allow for inbuilt force, torque and position sensing at each joint. Figure 1, shows the left arm of the Baxter Robot and labels all the joints associated with it. Here, S, E, and W stand for shoulder, elbow, and wrist respectively. For the rest of the paper, we will concern ourselves with the left arm of the Baxter Robot. Baxter Robot has 3 offsets due to which no 3 consecutive frames meet at the same origin. Therefore, according to *Piepers* Principle, Baxter does not have an analytical solution to the inverse pose kinematics. [1] The approach for the kinematic analysis of a redundant robotic Arm can be obtained from the work of *Dimo*, others [2] Performing tasks with a robotic manipulator require an understanding of its mathematical model. This includes both, its kinematic and dynamic models.

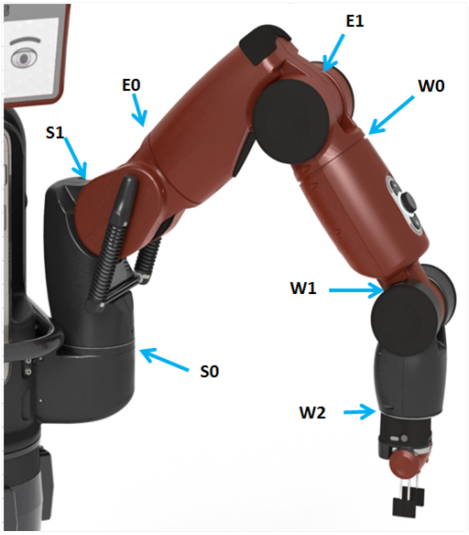

Fig. 1. The left arm of Baxter Robot

[1]A. Gandhi, A. Kumar, S. Dikhale are with the Human Inspired Robotics Lab, Robotics Engineering Program, Worcester Polytechnic Institute, Worcester MA 01609, USA { agandhi2,ssdikhale,archit } @ wpi.edu

A. Kinematics

Robot kinematics allows us to derive relations between all joints of the robot. The problem can be approached in two methods: forward kinematics, inverse kinematics. The forward kinematics problem is often simple in the case of serial manipulators. It allows us to locate the position of the robot end-effector, given the robot geometry and joint angles. There are multiple methods for deriving the forward kinematics of the system, the homogeneous transformation using Denavit-Hartenberg parameters being the most widely used methods. The inverse kinematics problem is not as easy for serial manipulators and in most cases does not have closed-form solutions. The inverse kinematic problem deals with finding the joint angles, given the geometry of the robot and the position of its end-effector. It is usually solved using a geometric or analytical approach. In this paper, we have used the geometric approach with certain assumptions to derive an inverse kinematic model for the redundant Baxter's arm.

B. Dynamics

The relationship between forces acting on a robot mechanism and the accelerations produced constitutes Robot Dynamics. In robot mechanism, dynamics is an application of rigid body dynamics to robots. The two problems of dynamics are forward dynamics where we are given the forces and we calculate acceleration and the other approach is inverse dynamics where we are given the acceleration and we work out the forces. The dynamical modeling of the system can be in two approaches. The first one is the Euler-Lagrange approach and the other is the Newton-Euler approach. The Euler-Lagrange model, the links are considered together and the model is obtained analytically using kinetic and potential energy of the system. The Newton-Euler method forms an equation with a recursive solution. In order to derive the dynamic model, we employed the Euler Lagrange method

wherein we calculated the Lagrangian(L) by subtracting the total potential energy(p) from the total kinetic energy(k) and then calculating the required derivatives and partial derivatives.

II. Methodology

The mathematical model for the system was developed from the information provided on the Baxter robot data sheet by Rethink Robotics[3]. Geometric calculations and MATLAB code were extensively used to create the model using the techniques learned in class.Simulations were coded in MATLAB and the outputs were screen recorded as video files, attached along with the submission. Experimental work was performed on the Baxter robot model in the HiRo lab at WPI. The kinematic model of Baxter was verified by reading joint angles from the robot console for specific poses and compared with our derived model.The rest of the report is organized as follows. Section III discusses the mathematical model of the robot. Experimental Results were obtained in Section IV and are followed by the Result and Conclusions.

III. Mathematical Model

A. Forward Kinematics

To obtain the forward kinematics solution for the Baxter Robot we use the Denavit-Hartenberg(DH) convention to calculate a final Homogeneous transformation matrix that relates the base frame to the end effector frame, giving us the position and orientation of the end effector. The coordinate frame assignment for the joints while following the DH conventions are shown in Figure 2. Table 1 below contains the DH parameters for the given robot model. The following equations give us the position of the end effector (x,y,z), in terms of joint angles.

$$
\begin{aligned}
\mathbf{x} = {} & a_1 cos\theta_1 - d_5(sin\theta_4(sin\theta_1 \\
& sin\theta_3 + cos(\theta_2 - 90)cos\theta_1 \\
& cos\theta_3) + sin(\theta_2 - 90)cos\theta_1 \\
& cos\theta_4) - d_7(cos\theta_6(sin\theta_4 \\
& (sin\theta_1 sin\theta_3 + cos(\theta_2 - 90) \\
& cos\theta_1 cos\theta_3) + sin(\theta_2 - 90) \\
& cos\theta_1 cos\theta_4) + sin\theta_6(cos\theta_5 \\
& (cos\theta_4(sin\theta_1 sin\theta_3 + cos(\theta_2 - 90) \\
& cos\theta_1 cos\theta_3) - sin(\theta_2 - 90)cos\theta_1 \\
& sin(\theta_4)) + sin\theta_5(cos\theta_3 sin\theta_1 \\
& - cos(\theta_2 - 90)cos\theta_1 sin\theta_3))) - a_5 \\
& cos\theta_5(cos\theta_4(sin\theta_1 sin\theta_3 \\
& + cos(\theta_2 - 90)cos\theta_1 cos\theta_3) \\
& - sin(\theta_2 - 90)cos\theta_1 sin\theta_4) \\
& - a_5 sin\theta_5(cos\theta_3 sin(\theta_1) \\
& - cos(\theta_2 - 90)cos\theta_1 sin\theta_3) - a_3 \\
& sin\theta_1 sin\theta_3 - d_3 sin(\theta_2 - 90) \\
& cos\theta_1 - a_3 cos(\theta_2 - 90)cos\theta_1 \\
& cos\theta_3
\end{aligned} \tag{1}
$$

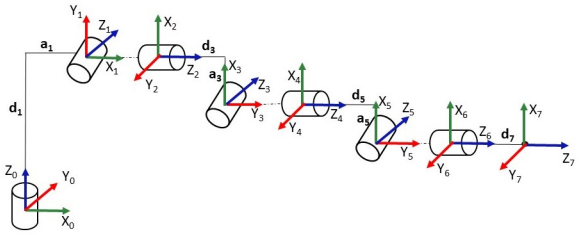

Fig. 2. Coordinate Frames Assigned in Link Diagram

$$
\begin{aligned}
\mathbf{y} = {} & d_7(cos\theta_6(sin\theta_4(cos\theta_1 sin\theta_3 \\
& - cos(\theta_2 - 90)cos\theta_3 sin\theta_1) \\
& - sin(\theta_2 - 90)cos\theta_4 sin\theta_1) \\
& sin\theta_3 - cos(\theta_2 - 90)cos\theta_3 sin\theta_1) \\
& + sin(\theta_2 - 90)sin\theta_1 sin\theta_4) \\
& + sin\theta_5(cos\theta_1 cos\theta_3 + sin\theta_5 \\
& (cos\theta_1 cos\theta_3 + cos(\theta_2 - 90) \\
& sin\theta_1 sin\theta_3))) + d_5(sin\theta_4 \\
& (cos\theta_1 sin\theta_3 - cos(\theta_2 - 90) \\
& cos\theta_3 sin\theta_1) - sin(\theta_2 - 90) \\
& cos\theta_4 sin\theta_1) + a_1 sin\theta_1 + a_5 \\
& cos\theta_5(cos\theta_4(cos\theta_1 sin\theta_3 \\
& sin\theta_1 sin\theta_4) + a_5 sin\theta_5 \\
& (cos\theta_1 cos\theta_3 + cos(\theta_2 - 90) \\
& sin\theta_1 sin\theta_3) + a_3 cos\theta_1 sin\theta_3 \\
& - d_3 sin(\theta_2 - 90)sin\theta_1 - a_3 \\
& cos(\theta_2 - 90)cos\theta_3 sin\theta_1
\end{aligned} \tag{2}
$$

$$
\begin{aligned}
\mathbf{z} = {} & d_1 - d_7(cos\theta_6(cos(\theta_2 - 90)cos\theta_4 \\
& - sin(\theta_2 - 90)cos\theta_3 sin\theta_4) \\
& - sin\theta_6(cos\theta_5(cos(\theta_2 - 90)sin\theta_4 \\
& + sin(\theta_2 - 90)cos\theta_3 cos\theta_4) \\
& - sin(\theta_2 - 90)sin\theta_3 sin\theta_5)) - d_5 \\
& (cos(\theta_2 - 90)cos\theta_4 - sin(\theta_2 - 90) \\
& cos\theta_3 sin\theta_4) - d_3 cos(\theta_2 - 90) \\
& sin\theta_4 + sin(\theta_2 - 90)cos\theta_3 cos\theta_4) \\
& + a_3 sin(\theta_2 - 90)cos\theta_3 - a_5 \\
& sin(\theta_2 - 90)sin\theta_3 sin\theta_5
\end{aligned} \tag{3}
$$

TABLE I
DH PARAMETERS FOR BAXTERS LEFT ARM

Link	$\theta(deg)$	d	a	α
1	θ_1^*	d_1	a_1	-90°
2	$\theta_2^* - 90°$	0	0	-90°
3	θ_3^*	d_3	$-a_3$	90°
4	θ_4^*	0	0	90°
5	θ_5^*	d_5	$-a_5$	90°
6	θ_6^*	0	0	-90°
7	θ_7^*	d_7	0	0

Where:
d_1= 270.35 mm
d_3= 364.35 mm
d_5= 374.29 mm
d_7= 229.525 mm
a_1= 69 mm
a_3= 69 mm
a_5= 10 mm

B. Workspace

The tables 2 and 3 lists the range of motion of the joints of "Baxter". These joints are divided into two categories namely "Bend" and "Twist" joints. They have varying ranges of motion, with the twist joints having a relatively higher freedom in movement. Figure 3 shows the skeletal model of the left arm of the robot. Figure 4 shows a plot of the reachable workspace of the left arm. A video of the simulation of the workspace plot is attached.

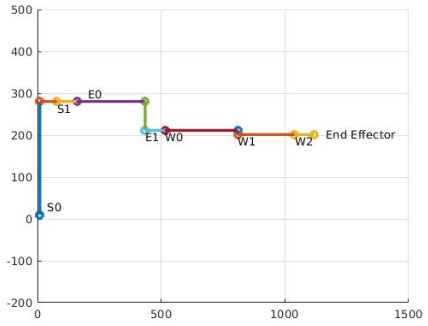

Fig. 3. Coordinate Frames Assigned in Link Diagram

TABLE II
RANGE OF MOTION FOR BEND JOINTS

Joint	$\theta(min)$	$\theta(max)$	Range
S1	-123°	+60°	183°
E1	-2.864°	+150°	153°
W1	-90°	+120°	210°

TABLE III
RANGE OF MOTION FOR TWIST JOINTS

Joint	$\theta(min)$	$\theta(max)$	Range
S0	-97.494°	+97.494°	194.998°
E0	-174.987°	+174.987°	349.979°
W0	-175.25°	+175.25°	350.5°
W2	-175.25°	+175.25°	350.5°

C. Inverse Kinematics

To simplify the inverse kinematics solution for the Baxter robot, the following assumptions were made.

- Joint E0 is fixed

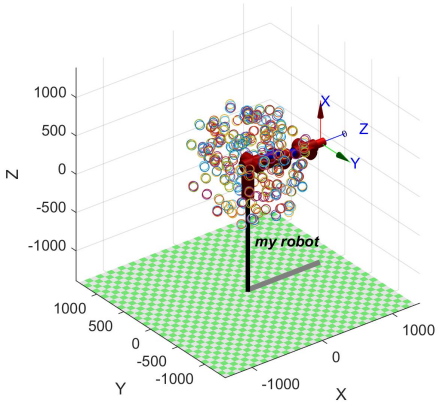

Fig. 4. Baxter's left arm workspace plot

- Assumed length of link a5 = 0, as it is negligible as compared to that of other links

Fixing Joint E0 allows us to consider the redundant manipulator as a 6 DoF manipulator thus making it possible to compute the inverse kinematics of the structure. Assuming the length of link a5 to be zero, renders joints W0, W1 and W2 to form a spherical wrist thus allowing us to decouple the manipulator and solve for its inverse kinematics very easily. We know the position of the end effector from the forward kinematics of the robot. This can be used to solve the inverse position kinematics, i.e: the first three joint angles.

$$\theta_{\mathbf{1}} = \pi + atan2(x_c, y_c) \tag{4}$$

$$\theta_{\mathbf{2}} = atan2(r, s) - atan2(l_3 + d_5 cos\theta_3, d_5 sin\theta_3) \tag{5}$$

$$\theta_{\mathbf{3}} = cos^{-1}(D) \tag{6}$$

where,

$$\mathbf{D} = \frac{r_2 + s_2 - l_3^2 - d_5^2}{2 l_3 d_5} \tag{7}$$

$$\mathbf{r} = x_c^2 + y_c^2 \tag{8}$$

$$\mathbf{s} = z_c - d_1 \tag{9}$$

These angles are then used to find the position of the wrist center and the remaining three angles can be found by using the Euler angles method.

$$\theta_{\mathbf{4}} = atan2(-cos\theta_4 sin\theta_5, -sin\theta_4 sin\theta_5) \tag{10}$$

$$\theta_{\mathbf{5}} = atan2(cos\theta_5, \sqrt{1 - cos^2\theta_5}) \tag{11}$$

$$\theta_{\mathbf{6}} = atan2(-cos\theta_6 sin\theta_5, -sin\theta_5 sin\theta_6) \tag{12}$$

D. Velocity Kinematics

Another important part of formulating the Kinematic solution for a robot serial manipulator is determining the "Velocity Kinematics". This involves developing a relation between joint velocities and end effector velocity i.e between the joint and task space respectively. We have the following velocity kinematic equation,

$$\dot{\mathbf{x}} = J\dot{q} \tag{13}$$

This relation is determined by a "Jacobian matrix" (J). The Jacobian is used not only for obtaining a relation between joint and end effector velocities but also for relating joint torques and end effector forces, for finding the singularity of a robot manipulator(robot configurations that result in the elimination of one or more DoF), planning trajectories etc. The Jacobian matrix is a 6 by n matrix, "n" being the number of links. If we have a square Jacobian then we can easily determine the inverse of the Jacobian when looking to find the joint velocity matrix. However when we do not have a square jacobian matrix, we find a Pseudo inverse for the Jacobian which gives us the matrix closest to the actual inverse of the non-square Jacobian. Our calculated Jacobian is a matrix of order 6x7, which means we had to calculate the pseudo inverse of the Jacobian to calculate the joint velocities given the end effector velocity.

$$\dot{\mathbf{q}} = J^{+}\dot{x} \tag{14}$$

E. Dynamics

In order to formulate the dynamic model for Baxter we used the Euler-Lagrange method. An important point to be noted is that we are assuming the links to be massless and only accounting for point masses at the end of each respective link. This means we calculate only the translational part of kinetic energy and not the rotational part of kinetic energy.

$$\mathbf{L} = K.E. - P.E. \tag{15}$$

Differentiating the positions we obtain velocities which is then used to obtain the kinetic energy associated with each mass. Also, using the z-coordinate of each mass, respective potential energies are calculated. This gives us the Lagrangian, a crucial step in formulating the dynamic model using Euler-Lagrange. Substituting the required values into the Euler Lagrange equation gives us the dynamic model for Baxter's left arm manipulator.

$$\tau = \frac{d}{dt}\frac{\partial L}{\partial \dot{q}} - \frac{\partial L}{\partial q} \tag{16}$$

Additionally by taking terms common we arrive at the Inertia matrix(M), Gravity matrix(G) and the Coriolis Centripetal Coupling Vector(C).

$$\tau = M(q)\ddot{q} + C(q,\dot{q})\dot{q} + G(q) \tag{17}$$

TABLE IV

BAXTER JOINT ANGLE READINGS

Joint	Point 1(rad)	Point 2(rad)	Point3(rad)
E0	-0.1457	-0.0889	-0.1928
E1	1.7932	0.7393	1.0764
S0	-0.2477	-0.7666	-1.2969
S1	-0.8590	-0.3462	-0.4966
W0	0.1560	0.1698	0.2354
W1	0.6853	1.1723	1.0415
W2	0.4563	0.0195	0.2672

TABLE V

EXPERIMENTAL RESULTS

Point	Measured values(mm)	FK values(mm)	Error(%)
Point 1	124.00	-131.00	5.6
	67.06	69.00	2.9
	-601.90	-588.00	2.3
Point 2	633.46	-639.00	0.8
	-110.99	119.00	7.2
	-400.21	-414.50	3.5
Point 3	439.63	-435.80	0.8
	-85.55	-87.00	1.6
	-538.48	-549.00	1.9

IV. EXPERIMENT

Having formulated the mathematical model we sought to validate our work by performing an experiment to check for the kinematic solution. First we laid out three arbitrary points in the robot's workspace, and measured their cartesian positions with respect to joint E0 of the robot's left arm manipulator. Then, we moved the manipulator to the locations of the three points that we marked earlier. Using the Baxter API on ROS, we published joint angle values. These joint angles were then substituted in our forward kinematics solution, giving us the end effector position with respect to the base frame (at joint E0). Both sets of end effector positions, i.e those obtained from our forward kinematics equations and those from measured values in the cartesian space were then compared. This was performed for three different points in the workspace of the robot.

V. RESULTS AND DISCUSSIONS

While it was fairly easy to arrive at the forward kinematics solution for the robot, the inverse kinematics posed a challenge since we have a seven DoF robot with offsets. However making a few assumptions we were able to formulate a solution to the inverse problem as well.

Also to relate the joint and end effector velocities we were able to come up with the Jacobian, size 6 by 7, which is a non-square matrix. The challenge of calculating the inverse was solved by considering the "Moore-Penrose" or the "Pseudo-inverse" Jacobian to come up with a close approximation of the actual inverse for the non-square Jacobian matrix.

The dynamic modelling of the robot was also successfully performed using the Euler-Lagrange method.

Table 4, shows the joint angles in radians published via

the Baxter API on ROS for each of the three experimental points.The Table 5 compares experimental results with results from our simulations for all three points. The error computed was less than 7 percent, which is a good standard, considering that measurements were taken by hand and had the possibility of some inaccuracy.

VI. Conclusion And Future Work

Performing the kinematic and dynamic analysis of the Baxter robot has been a learning experience for us. It has helped us learn how to apply the theoretical concepts, studied in class, to a real world robot. Every robot's mechanism is different in the way that it offers a new challenge to analyze its design and come up with a solution to model its structure mathematically. Similarly, the "Baxter" robot being a redundant 7 DoF serial manipulator posed a complex problem, which was simplified by making certain assumptions in order to get a closed form solution and eventually arrive at its kinematic and dynamic model.

Having made this progress, our future goals entail planning the trajectory of the Baxter robot through the via points approach and graphically representing it in the form of time vs position, time vs velocity, and time vs acceleration plots. Also, it would be interesting to try and get one of the arms of "Baxter" to do useful tasks such as picking and placing an object or getting it to move while avoiding collision through an obstacle laden path. These future goals would certainly allow us to further reinforce our concepts.

References

[1] R.L. Williams II,Baxter Humanoid Robot Kinematics,Internet Publication,https://www.ohio.edu/mechanical-faculty/williams/html/pdf/BaxterKinematics.pdf,April 2017.

[2] H. O. Dimo, Dewen Jin; Jichuan Zhang(2002)."Optimal configuration of a redundant robotic arm: Compliance approach". Pp 281 - 285, Volume 7, Number 3, June 2002.

[3] Rethinkrobotics.com, 'Hardware Specifications', 2015. [Online] Available: http://sdk.rethinkrobotics.com/wiki/Hardware-Specifications.[Accessed: 14- Dec- 2018].

[4] Ju. Zhangfeng, Yang. Chenguang, Ma. Hongbin(2014),"Kinematics modeling and experimental verification of baxter robot." https://www.ohio.edu/mechanical-faculty/williams/html/pdf/BaxterKinematics.pdf,-8523. 10.1109/ChiCC.2014.6896430.

[5] L. E Silva, T. M. Tennakoon, M. Marques, and A. M. Djuric, "Baxter Kinematic Modeling, Validation, and Reconfigurable Representation", 2016, vol. 2016, April.

[6] A. Smith, C. Yang, C. Li, H. Ma, and L. Zhao, "Development of a dynamics model for the Baxter robot", in 2016 IEEE International Conference on Mechatronics and Automation, IEEE ICMA 2016, 2016, pp. 12441249.

[7] Chiaverini S., Oriolo G., Walker I.D. (2008) "Kinematically Redundant Manipulators". In: Siciliano B., Khatib O. (eds) Springer Handbook of Robotics. Springer, Berlin, Heidelberg.

[8] Mark W. Spong, Seth Hutchinson, and M. Vidyasagar. "Robot Dynamics and Control".